PERGAMON

Chaos, Solitons and Fractals 15 (2003) 695–711

CHAOS
SOLITONS & FRACTALS

www.elsevier.com/locate/chaos

Oscillation types, multistability, and basins of attractors in symmetrically coupled period-doubling systems

B.P. Bezruchko *, M.D. Prokhorov, Ye.P. Seleznev

Department of Saratov, Institute of Radio Engineering and Electronics of Russian Academy of Sciences, Zelyonaya Str., 38, Saratov 410019, Russia

Accepted 31 May 2002

Abstract

Symmetrically coupled nonlinear oscillator systems demonstrating transition to chaos via a sequence of period-doubling bifurcations under variation of the control parameter exhibit various types of mutual synchronization. For these coupled systems, with dissipatively coupled logistic maps, we consider a hierarchy of possible oscillation types using the value of the time shift between oscillations of the subsystems as a basis for the classification of multistable states. For oscillation states and their basins of attraction the ways of evolution are studied under variation of the parameters of nonlinearity and coupling. The obtained results are compared with those of physical experiment with a system of coupled, periodically driven nonlinear resonators.

1. Introduction

A system of two identical symmetrically coupled objects demonstrating transition to chaos via a sequence of period-doubling bifurcations under variation of the control parameter is one of the standard objects in nonlinear dynamics. The most detailed investigation of these coupled systems was carried out using discrete models in the form of coupled one-dimensional unimodal maps with quadratic maxima. It was shown that identical coupled maps demonstrate a variety of nonlinear phenomena, including multistability, synchronization, chaos and hyperchaos, frequency locking, intermittency, and crisis of chaotic attractors. The transition to chaos in such systems can be observed via a sequence of period-doubling bifurcations, as well as via a sequence of Hopf bifurcations [1–7]. The system parameter space has a complicated self-similar structure [8,9], whose universality can be explained by means of renormalization theory [8,10,11]. A variety of multistable states in coupled map system is very great [10,12–17]. Studying the basins of attraction of these states helps in understanding the ways of multistability formation [18–21]. The features of the complicated dynamics of the coupled systems that were revealed by maps investigation agree well with the results of experimental studies for various systems of coupled objects [4,12,13,21–24]. Coupled maps are quite popular in the context of studying the actual problems of loss of chaos synchronization and transition from synchronous to asynchronous chaotic motion [25–28]. In recent years they helped to explain the bifurcation mechanism of the loss of stability of the synchronous chaotic regime induced by the bubbling and riddling transitions in the system [29–34].

In spite of a large number of papers devoted to a system of two symmetrically coupled maps, the variety of types of mutual synchronization of subsystems and the hierarchy of stable oscillation states have not been adequately explored. The advisability of their consideration is determined by the fact, that branching of the hierarchy scheme and the variety

* Corresponding author. Fax: +7-8452-241156.
E-mail address: sbire@sgu.ru (B.P. Bezruchko).

0960-0779/03/$ - see front matter
PII: S0960-0779(02)00171-6

of multistable oscillations are so great, that sometimes even statistical approach is used for their description [35]. This testifies that the detailed description of complicated dynamics of symmetrically coupled systems deserves attention.

In this paper, with two dissipatively coupled quadratic maps as an example (Section 2), we suggest a classification of oscillation types for the coupled system based on the phase shift of subsystem oscillations. The regions of existence of multistable states in the parameter space and their evolution scheme for small values of coupling coefficient are presented in Section 3. In Section 4 the out-of-phase regimes existing in the region of strong coupling are examined. In Section 5 we investigate the evolution of basins of attraction for periodic and chaotic multistable states under variation of parameters. In Section 6 the obtained results are compared with those of physical experiment with a system of coupled nonlinear resonators. Section 7 contains discussion.

2. Object of investigation

All possible variants of symmetric coupling between identical maps with quadratic maxima can be represented by a combination of two basic types of coupling: dissipative and inertial [8,10]. In spite of some characteristic features inherent to each of these types of coupling, the commonness of oscillation motions in systems with dissipative and inertial coupling is large enough, what allows us to consider in detail only one of these types. In our paper the system of two coupled maps is examined for the case of dissipative coupling as an example. This type of coupling favours the equalization of the subsystem instantaneous states, and it has no influence on the system dynamics if these states are equal. Such type of coupling arises in many systems; for instance, in radiotechnical objects it is realized by means of a resistor. The system of dissipatively coupled maps can be written as

$$\begin{aligned} x_{n+1} &= f(x_n) + k[f(y_n) - f(x_n)], \\ y_{n+1} &= f(y_n) + k[f(x_n) - f(y_n)], \end{aligned} \tag{1}$$

where x, y are the dynamical variables, $n = 0, 1, 2, \ldots$ is the discrete time, $f(x_n)$ and $f(y_n)$ are the functions describing the behavior of isolated subsystems, k is the coupling coefficient. This form of coupling can be clearly interpreted by the example of population dynamics. One can think of $f(x_n)$ and $f(y_n)$ as simulating the population dynamics of a particular species at two adjacent locations. If the species can migrate in both directions within the time intervals between the stages of their reproduction and death, then k is the fraction of these species, which migrate to the neighbouring location. In this case the coupling parameter k can vary between zero and unity. In this interval of k variation the phase volume suffers additional contraction in comparison with the magnitude it would have without coupling. This fact gives grounds to call this type of coupling as dissipative.

We study the system (1) for the case $f(x_n) = \lambda - x_n^2$, $f(y_n) = \lambda - y_n^2$, where λ is the parameter of nonlinearity. As a result, the system (1) takes the following form

$$\begin{aligned} x_{n+1} &= \lambda - x_n^2 + k(x_n^2 - y_n^2), \\ y_{n+1} &= \lambda - y_n^2 + k(y_n^2 - x_n^2). \end{aligned} \tag{2}$$

We consider the case, where the values of λ are the same in both subsystems.

3. Classification of coupled system states and their evolution for weak coupling

3.1. Classification of oscillation types

By virtue of the fact that maps (1) are invariant with respect to the discrete group of symmetries, it is convenient to use the magnitude of the time shift between subsystem oscillations as a basis for the regimes classification. It is obvious that in the case of identical unimodal functions $f(x_n)$ and $f(y_n)$ each period-N regime of the system (1) can be realized in the limiting case of zero coupling ($k = 0$) by N variants differentiated by the time shift of the subsystem oscillations by $m = 0, 1, 2, \ldots, N-1$. We call them as oscillation types and use these types as a basis to describe the hierarchy of oscillation regimes as coupling is introduced, when the subsystems interaction leads to various variants of their mutual synchronization. Let us denote periodic regimes as N_m. The similar principle of classification can be used for chaotic regimes denoted as N^m, in spite of the lack of periodicity in their motion. In this case N should be read as denoting the number of bands (connectivity) of the attractor, and the superscript m is the time shift between oscillations of the subsystems at a certain band of the attractor, which, for instance, contains the maximum values of x_n and y_n. The regimes with $m = 0$, for which $x_n - y_n = 0$ and the phase portrait is located along the diagonal in the (x_n, y_n) plane, represent the in-phase states. The other oscillation regimes with $m \neq 0$ are out of phase. Note that chaotic regimes can

be out of phase ($x_n \neq y_n$) even at $m = 0$, for example, in the region of weak coupling. To distinguish these regimes from the in-phase ones we use the superscript $m = N$ for their notation. The realization of one or another oscillation type is defined by the parameter values and the choice of initial conditions.

3.2. Evolution scheme for small values of coupling coefficient

By depicting every multistable oscillation type lying on a separate sheet one can build a pictorial scheme of the regions of existence for stable oscillation regimes in the coupling coefficient–driving parameter plane. In Fig. 1 such scheme is presented for low-period regimes for $k < 0.5$. The phase portraits of these regimes and of chaotic regimes evolved from them are shown in Fig. 2(a), which is the section of Fig. 1 with the plane $k = \text{const}$ extended to the region of large λ values. This scheme illustrates qualitatively the evolution of motions of the system (2) with the parameter λ variation for fixed weak coupling. Let us consider the coupled system dynamics using another variant of the evolution scheme (Fig. 2(b)). The solid lines in this scheme correspond to the stable regimes and the dashed lines to the unstable ones. The bifurcation transitions are marked by the points. Let us explain the main components of this scheme. The branches A, B, C, and D indicated in the scheme combine certain groups of regimes. The branches begin with periodic regimes and end with chaotic ones. The branch A refers to evolution of the in-phase regimes with $m = 0$. The branches B, C, and D leaving from A correspond to the out-of-phase regimes. The branch B begins with period-2 cycle and combines oscillations with $m = 2l - 1$, $l = 1, 2, 3, \ldots$, branch C begins with period-4 cycle and combines oscillation types with $m = 2(2l - 1)$, and branch D begins with period-8 cycle and combines oscillations with $m = 4(2l - 1)$.

The values of λ, at which period-doubling bifurcations of in-phase cycles take place in the coupled system, coincide with the corresponding bifurcation values in the isolated subsystems. At the branching points of A the initial in-phase cycle loses its stability (one of its eigenvalues becomes equal to -1) and a stable in-phase cycle with doubled period appears in its neighbourhood, which extends the branch A. With λ increasing the cycle having lost its stability undergoes the period-doubling bifurcation once again (the second eigenvalue becomes equal to -1), and an unstable out-of-phase cycle with doubled period appears, which becomes stable later on. As a result, with the increase of λ each in-phase cycle $(2^n)_0$ gives rise to a pair of cycles, which involves an in-phase $(2^{n+1})_0$ and an out-of-phase $(2^{n+1})_{2^n}$ cycles. Out-of-phase cycles $2_1, 4_2, 8_4, \ldots$ emerging in this manner form the basis of branches B, C, D, ... and, with λ increasing, they of necessity undergo a Hopf bifurcation followed by a quasiperiodic motion. As the result of frequency locking, the following pairs of out-of-phase cycles appear: 4_1 and 4_3 on branch B, 8_2 and 8_6 on branch C, 16_4 and 16_{12} on branch D. Each of these cycles in turn give rise to two cycles similarly to the considered case of in-phase cycles. This process is continued up to the critical λ values corresponding to the formation of a chaotic attractor from every cycle of the

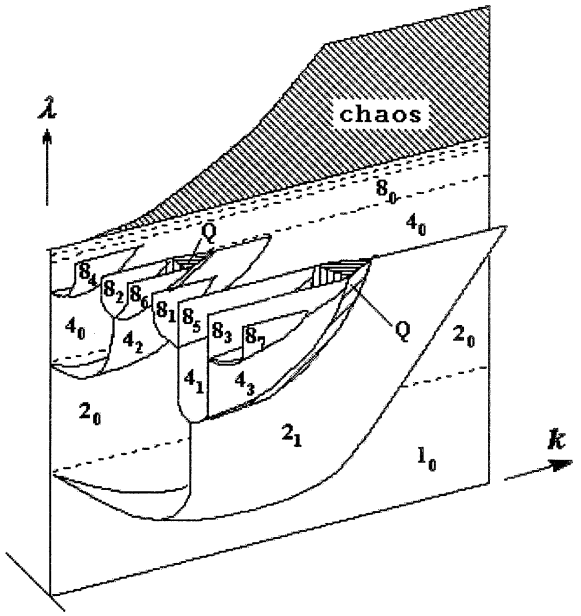

Fig. 1. Qualitative scheme of the (k, λ) plane for system (2), representing regions of existence for all oscillation regimes of periods 1, 2, 4, and 8 for $k < 0.5$. Regions of quasiperiodic regimes are denoted by Q.

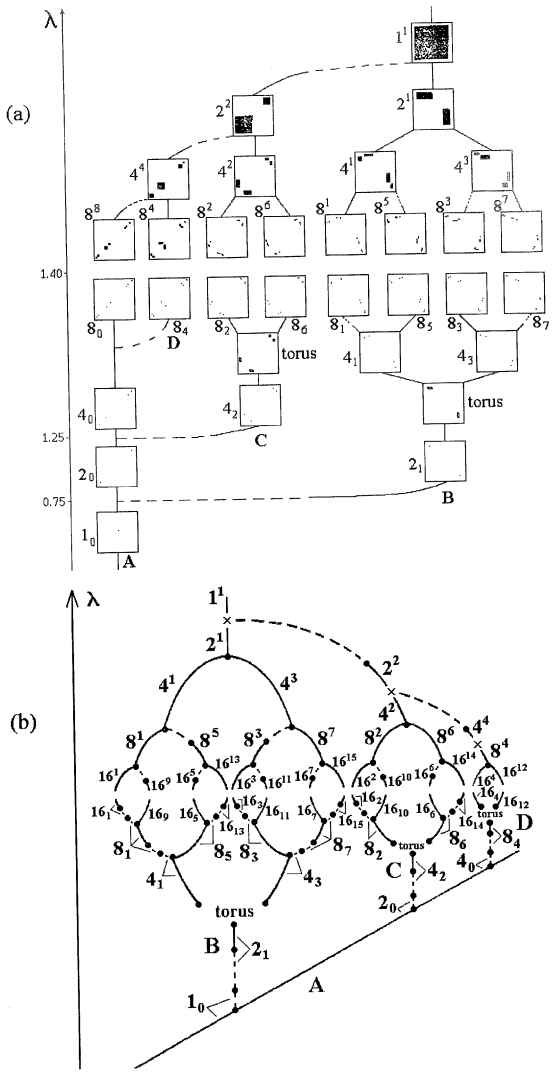

Fig. 2. (a) Attractors of the system (2) in the (x_n, y_n) plane for $k = 0.006$. (b) Evolution scheme for oscillation states of the coupled system under variation of the control parameter at a fixed small coupling coefficient.

branch. In the region of chaos the evolution scheme is superficially similar to the scheme of periodic regimes. The dashed lines correspond to nonattracting sets and the solid lines refer to chaotic attractors. The points of dashed and solid lines merging correspond to the attractor bands merging and union of the attractor and previously nonattracting set. As a result, an attractor containing the both above mentioned sets is formed. With the increase of λ each branch is ended by a pair of chaotic attractors having the same indices as the cycles which emerged as the result of frequency locking (4^1 and 4^3 on branch B, 8^2 and 8^6 on branch C, and so on). With further increase of the parameter λ the regime of chaos–chaos intermittency is observed between the attractors of the pair. The regime of intermittency is softly replaced by attractor $(2^n)^m$ with n and m being equal to the indices of the cycle beginning this branch: 2^1 on branch B, 4^2 on branch C, and so on. Above the mark $\times$ the corresponding attractor combines with the attractors produced by the branches located at the right of Fig. 2(b).

At zero coupling and λ values below the critical value the oscillations of identical subsystems are the same and they can be only shifted in time relative to each other. Nonzero coupling leads to the difference in temporal realizations of periodic oscillations even for identical subsystems and to the break of symmetry for the cycle with respect to the exchange $x \leftrightarrow y$. This is true for all oscillation types except the in-phase ones $(2^n)_0$ and the types $(2^{n+1})_{2^n}$ emerged directly from the in-phase types. The distinction grows as coupling increases, but it does not affect the determining criterion for the os-

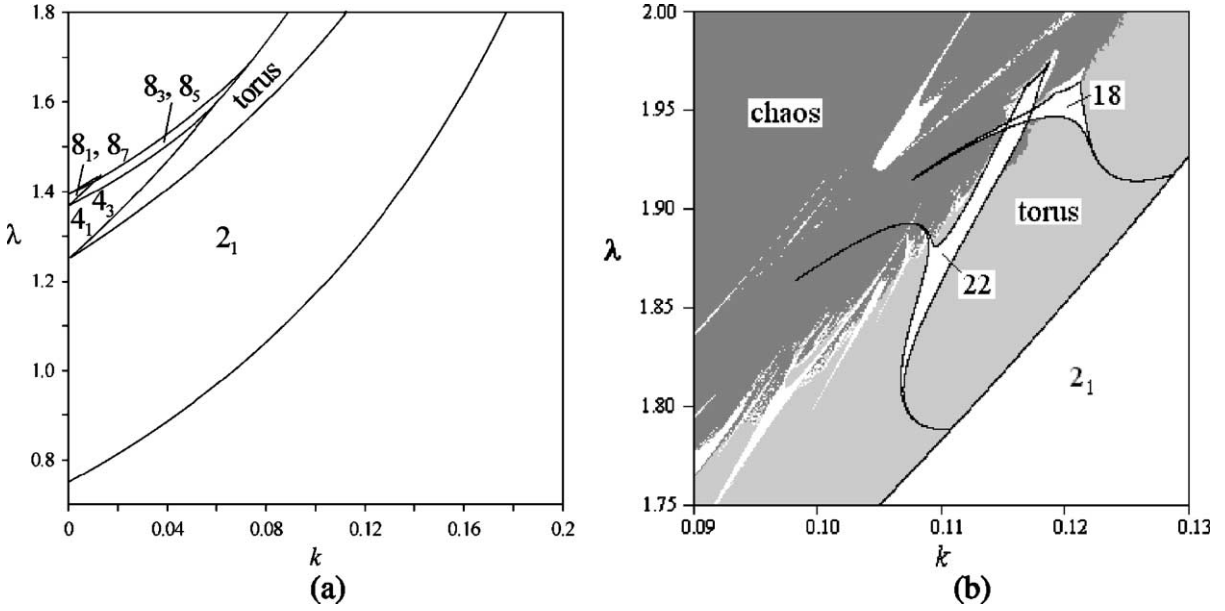

Fig. 3. (a) Regions of stability of out-of-phase cycles in the branch B of the evolution scheme. (b) Regions of existence of the resonance cycles of periods 18 and 22.

cillation type, namely, the fixed value of time shift between the subsystem oscillations (if by this is meant the time interval, for instance, between the maxima of periodic realizations x_n and y_n). The cycles emerged as the result of frequency locking form the specular symmetric pairs: 4_1–4_3, 8_2–8_6, 16_4–16_{12}, ... These cycles are transformed one to another under the exchange $x \leftrightarrow y$. The cycles emerged from these ones also form the specular symmetric pairs $(2^n)_m - (2^n)_{2^n-m}$ under the condition of identity of evolution routes. For example, the specular symmetric types are 8_1–8_7, 16_2–6_{14}, 16_1–16_{15}, emerged after period doubling of cycles having lost their stability, and the types 8_5–8_3, 16_{10}–16_6, emerged directly as the result of the period-doubling bifurcation of initial cycle (Fig. 2(b)). As it can be seen from Figs. 1 and 3(a), the out-of-phase oscillation types existing in the region of weak coupling lose their stability as parameter k increases.

With λ increasing all out-of-phase symmetric cycles N_m, $m = N/2$, undergo Hopf bifurcation (the eigenvalues of these cycles become complex conjugate and reach the unity by absolute value). Besides quasiperiodic motions, a set of resonance cycles takes place as the result of frequency locking. They have the even periods and the typical shape in the form of tongue. The regions of two such resonance cycles with periods of 18 and 22 are presented in Fig. 3(b). These cycles are symmetric with respect to the exchange $x \leftrightarrow y$ and demonstrate Hopf bifurcation, followed by quasiperiodic motion (the secondary torus) under the parameters variation. Close to the region of existence of the secondary torus a set of resonance cycles is also observed. It is rather difficult to define specific features of their hierarchy. However, it should be noted that in this region the symmetric resonance cycles are found, which in turn demonstrate Hopf bifurcation under variation of the parameters. Thus, moving along a complicated trajectory in the parameter space of the system under investigation, one can observe a sequence of transitions: cycle–torus–resonance cycle–torus–resonance cycle–torus.

Asymmetric, but symmetric to each other cycles, for example, 4_1 and 4_3 (the exchange $x \leftrightarrow y$ transfers them one to another) emerge as the result of saddle-node bifurcation. The lines of saddle-node bifurcations for these cycles coincide and bear up against the line of Hopf bifurcation at the point $k = 0$ (Fig. 3(a)). The occurrence of one or another cycle depends on the choice of initial conditions. The structure of the parameter plane depicted in Fig. 3(a) is typical for all branches of out-of-phase regimes.

The considered evolution scheme for small values of coupling coefficient (Fig. 2(b)) is typical for coupled systems (1) with identical unimodal functions.

4. Out-of-phase regimes at strong coupling

In the region of strong coupling $(0.5 \leqslant k \leqslant 1)$ the sheet of the in-phase oscillations in the (k, λ) plane is continued without peculiarities (Fig. 4(a)). As for the sheets, corresponding to the out-of-phase oscillation types, their arrangement

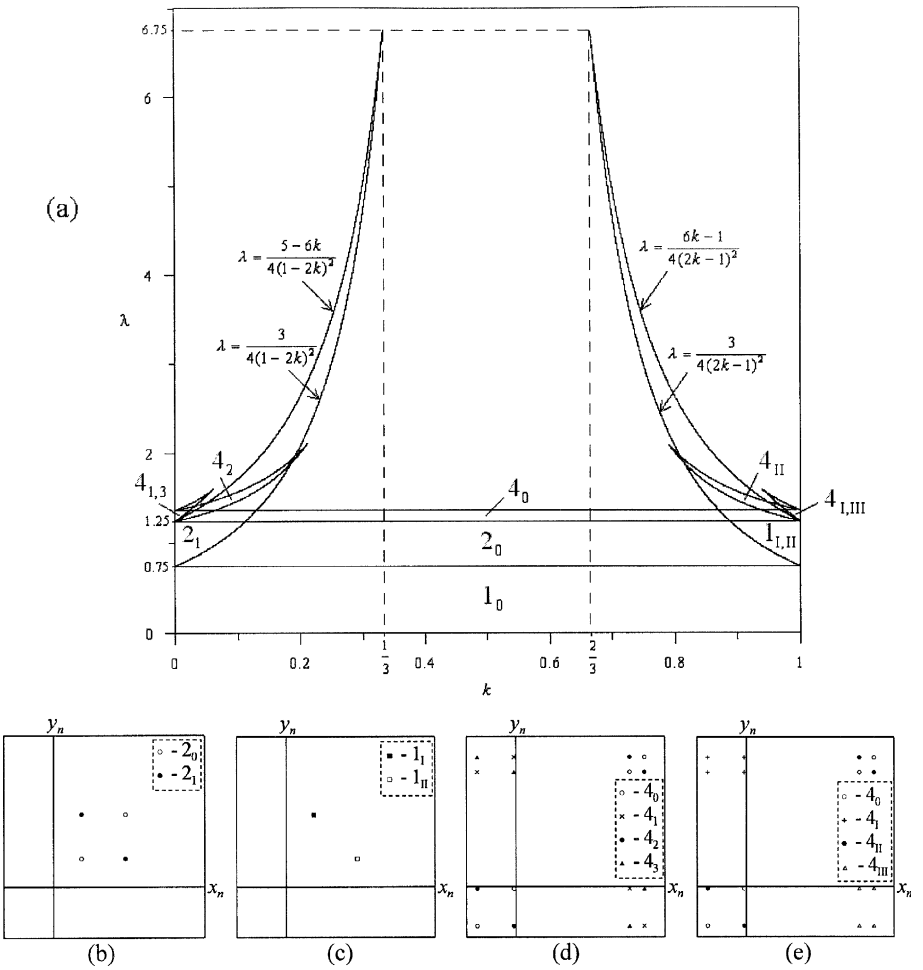

Fig. 4. (a) Regions of stability for period-1, 2, 4 cycles in the (k, λ) plane of the system (2). For out-of-phase period-1 and period-2 cycles the boundaries of the regions are deduced in the explicit form. (b,c) Attractors of periods 2 and 1 for $\lambda = 0.8$ and $k = 0, 1$, respectively. (d,e) Attractors of period 4 for $\lambda = 1.3$ and $k = 0, 1$, respectively.

is entirely symmetric with respect to the line $k = 0.5$ (see Fig. 4(a)). However, despite the symmetry of bifurcation lines, the out-of-phase regimes are radically different at weak and strong coupling. We use the Roman figures to denote the indices for the out-of-phase regimes at strong coupling. The stable out-of-phase period-1 cycles exist in the region of strong coupling. Their existence can be demonstrated in the following way: let us enter the new variables $u_n = (x_n - y_n)/2$, $v_n = (x_n + y_n)/2$. In these new variables the system (2) will be written in the form

$$\begin{aligned} u_{n+1} &= 2(2k-1)u_n v_n, \\ v_{n+1} &= \lambda - v_n^2 - u_n^2. \end{aligned} \tag{3}$$

For the period-1 cycle $u_{n+1} = u_n = u, v_{n+1} = v_n = v$, and from system (3) it follows

$$\begin{aligned} &u(1 - 2(2k-1)v) = 0, \\ &v^2 + v + u^2 - \lambda = 0. \end{aligned} \tag{4}$$

The first equation in (4) has two solutions: $u = 0$ and $v = 1/2(2k-1)$. The case of $u = 0$ corresponds to the in-phase regime $(x_n = y_n)$, and from the second equation it follows $v_{1,2} = (-1 \pm (1 + 4\lambda)^{1/2})/2$. The second solution corresponds to the out-of-phase regime. Substituting v into the second equation of the system (4) gives $u_{1,2} = \pm(\lambda - (4k-1)/(4(2k-1)^2))^{1/2}$.

To examine the stability of period-1 cycles we find their multipliers as eigenvalues of the Jacobian matrix M of the map (3)

$$M = \begin{bmatrix} 2(2k-1)v & 2(2k-1)u \\ -2u & -2v \end{bmatrix}.$$

Denoting the period-1 cycle multipliers by $\mu_{1,2(1)}$ we obtain

$$\mu_{1,2(1)} = 2v(k-1) \pm 2\sqrt{k^2v^2 + u^2(1-2k)}. \tag{5}$$

For the in-phase cycle 1_0: $u = 0$ and $\mu_{1(1_0)} = -2v$, $\mu_{2(1_0)} = 2v(2k-1)$. Thus, in the interval of positive λ the value $v_1 = (-1-(1+4\lambda)^{1/2})/2$ corresponds to the always unstable fixed point, and $v_2 = (-1+(1+4\lambda)^{1/2})/2$ relates to the stable (for $\lambda < 3/4$) fixed point (the both multipliers are less than unity by the absolute value).

Substituting the v and $u_{1,2}$ values, corresponding to the out-of-phase regime, into (5) and denoting multipliers at points (v, u_1) and (v, u_2) by $\mu_{1,2(1_I)}$ and $\mu_{1,2(1_{II})}$, respectively, yield

$$\mu_{1,2(1_I)} = \mu_{1,2(1_{II})} = \frac{k-1}{2k-1} \pm \sqrt{\left(\frac{k-1}{2k-1}\right)^2 + \frac{4\left(k-\lambda(2k-1)^2\right)}{2k-1}}. \tag{6}$$

Thus, the two out-of-phase period-1 cycles, symmetric about the change $u \to -u$ (or $x \leftrightarrow y$) exist and they always have equal multipliers. These cycles are stable in a wide range of parameters (see Fig. 4(a) in which the boundaries of the region of stability for cycles 1_I and 1_{II} are deduced in the explicit form from (6)). For instance, as $k = 1$: $\mu_{1,2(1_I)} = \mu_{1,2(1_{II})} = \pm 2(1-\lambda)^{1/2}$ and cycles 1_I, 1_{II} are stable at $3/4 < \lambda < 5/4$, i.e., at the same parameter values as the period-2 cycle in the uncoupled system.

The symmetry of the system (2) bifurcation lines with respect to $k = 0.5$, i.e., under the change $k \to 1-k$, can be confirmed by the cycle multipliers analysis. We show it with the out-of-phase period-1 and period-2 cycles as an example. For the period-2 cycle the Jacobian matrix of the map (2) has the form

$$M = \begin{bmatrix} 2x_1(k-1) & -2ky_1 \\ -2kx_1 & -2y_1(k-1) \end{bmatrix} \begin{bmatrix} 2x_2(k-1) & -2ky_2 \\ -2kx_2 & -2y_2(k-1) \end{bmatrix}, \tag{7}$$

where x_1, x_2 and y_1, y_2 are the cycle elements in the subsystems x and y, respectively. The out-of-phase cycle 2_1 is symmetric and $x_1 = y_2$, $x_2 = y_1$ for it. With regard to this, the out-of-phase cycle 2_1 multipliers, which are the eigenvalues of the matrix (7), take the form

$$\mu_{1,2(2_1)} = 2k^2(x_1+y_1)^2 + 4x_1y_1(1-2k) \pm 2k(x_1+y_1)\sqrt{k^2(x_1+y_1)^2 + 4x_1y_1(1-2k)}. \tag{8}$$

By expressing the multipliers $\mu_{1,2(2_1)}$ only in terms of parameters λ and k, we obtain

$$\mu_{1,2(2_1)} = \frac{2k^2}{(1-2k)^2} + \frac{4(1-k-\lambda(1-2k)^2)}{1-2k} \pm \frac{2k}{1-2k}\sqrt{\left(\frac{k}{1-2k}\right)^2 + \frac{4(1-k-\lambda(1-2k)^2)}{1-2k}}. \tag{9}$$

Taking the square of (6) and denoting the multipliers of the out-of-phase cycles 1_I and 1_{II} as $\mu_{1,2(1_{I,II})}$, we finally obtain

$$\mu_{1,2(2_1)}(\lambda, k) = \mu^2_{2,1(1_{I,II})}(\lambda, 1-k). \tag{10}$$

Consequently, if $|\mu_{1,2(2_1)}(\lambda,k)| < 1$ (the out-of-phase cycle 2_1 is stable for a certain k), then $|\mu_{1,2(1_{I,II}}(\lambda, 1-k)| < 1$ (the out-of-phase period-1 cycles are stable for the coupling value $1-k$).

For an arbitrary k it is easy to show that the change $k \to 1-k$ in the system (2) leads to the change $x_{n+1} \leftrightarrow y_{n+1}$, which is equivalent to the symmetric reflection of the point (x_{n+1}, y_{n+1}) about the line $x = y$. As a result, if the cycles of period 2^n, $n = 2, 3, \ldots$, exist for some k value, then the cycles having the same period and type of symmetry take place for the coupling value equal to $1-k$. The phase portraits of the specular symmetric pairs of cycles $(2^n)_m - (2^n)_{2^n-m}$ are qualitatively different for coupling coefficients k and $1-k$, and the phase portraits of the out-of-phase symmetric cycles $(2^n)_{n/2}$ coincide outwardly, but differ by the order of the elements sequence (Fig. 4(b)–(e)).

It should be noted that the introduction of coupling between the elements results in the emergence of stable regimes existing at such parameter values, which are unattainable without coupling. For example, it is seen from Fig. 4(a), that the stable out-of-phase period-1 and period-2 regimes exist in the coupled system for λ values by more than three times higher than the critical value ($\lambda_{cr} = 2$), at which all in-phase solutions go to infinity. Hence, the introduction of coupling between elements not only enriches the system dynamics, but it can substantially extend the region of its finite solutions.

The considered features of out-of-phase regimes at strong coupling are common for a wide class of systems (1) under condition of identity of unimodal functions $f(x_n)$ and $f(y_n)$.

5. Basins of attraction of multistable states

Let us consider the features of basins formation with the model (2) as an example moving according to the scheme in Fig. 2(a) from bottom to top, from the λ values corresponding to the sole period-1 cycle in the phase space. In Fig. 5(a) the situation is illustrated, where the point C is the stable solution of the system (the period-1 cycle) and its basin of attraction occupies the entire region of x_0, y_0 values bounded by the straight lines $|x_0| = |x_B|$, $|y_0| = |y_B|$, where x_B, y_B correspond to the unstable solution (the point B). For $k = 0$ the basin is a square with the side $a = 1 + (1 + 4\lambda)^{1/2}$. With the coupling coefficient increasing the basin is gradually deformed taking the form of a circle with the radius $r = \sqrt{2}(1 + (1 + 4\lambda)^{1/2})$ (Fig. 5(b)). If the initial point (x_0, y_0) is located beyond the basin of attraction, the solution goes to infinity (in Fig. 5 and subsequent figures this region is shown by hatching). The system (2) is invariant with respect to the change $x_n \to -x_n$, $y_n \to -y_n$. Therefore, the basins of attractors are symmetric about the axes $x_0 = 0$, $y_0 = 0$, and in the following figures we depict only the right upper quadrant of the plane (x_0, y_0).

With the emergence of the second attractor in the phase space the region of finite solutions is divided into the basins of coexisting attractors. The principle of the basins division is explained by Fig. 6(a), plotted for the case $k = 0$ and the nonlinearity $\lambda > \lambda_1$ where λ_1 is the value of the first period-doubling bifurcation. The period-1 cycle (the point C) has already lost its stability and two attractors, period-2 cycles 2_0 and 2_1, coexist in the phase space (Figs. 6(a) and 1). The set of unstable points, including the point C with preimages of all ranks, forms the boundaries of basins of attraction for coexisting cycles. It should be noted that near the boundary of the region of finite solutions a fractal structure takes place, that illustrates the absence of restriction for the regions division (Fig. 6(b)). The parameter λ increasing results in

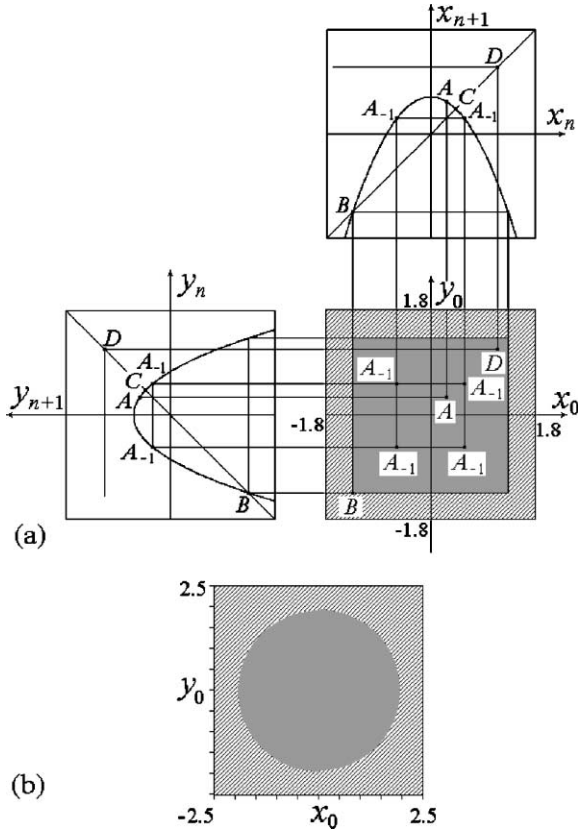

Fig. 5. Basin of attraction of period-1 cycle at $\lambda = 0.5$. (a) $k = 0$, (b) $k = 0.5$.

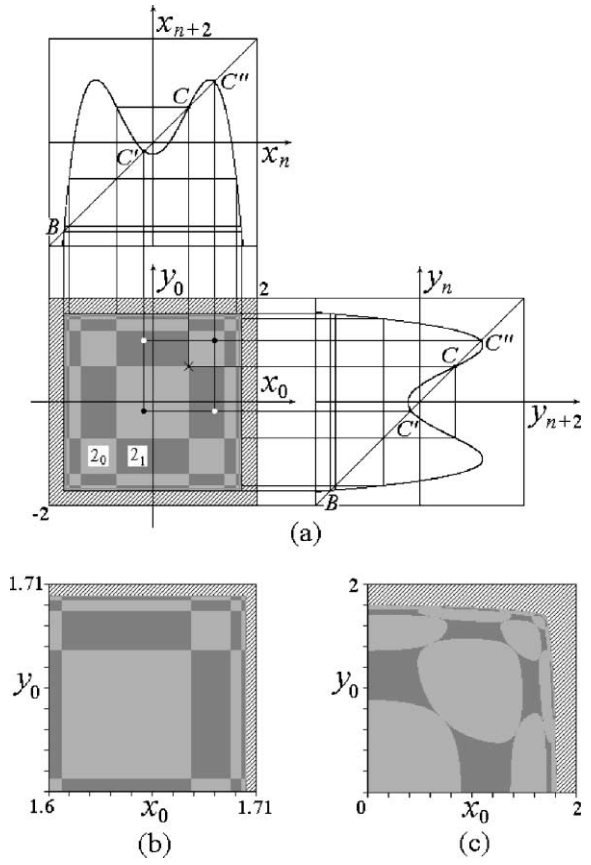

Fig. 6. (a) Plots of the second iterates $x_{n+2} = f(x_n)$ and $y_{n+2} = f(y_n)$ of the system (2) and basins of attraction of cycles 2_0 (•) and 2_1 (○) for $\lambda = 1.2$, $k = 0$. C is the unstable point (period-1 cycle (×)), C' and C'' are the stable points. (b) Enlarged fragment of (a) near the boundary of finite solutions. (c) Basins of attraction of period-2 cycles for $\lambda = 1.2$, $k = 0.08$.

period-doubling bifurcations followed by a greater number of coexisting regular attractors in the phase space. After each period-doubling bifurcation the in-phase cycle basin area is distributed among the basins of the in-phase and the symmetric out-of-phase cycles of the doubled period (for example, $2_0 \to 4_0$, 4_2; $4_0 \to 8_0$, 8_4). As for the basins of the out-of-phase cycles, they are divided into the basins of specular symmetric cycles (for example, $2_1 \to 4_1$, 4_3; $4_3 \to 8_3$, 8_7). In both cases the basin structure becomes fractal near the former boundaries (Fig. 7(b) and (c)). The basins division is continued up to the critical value $\lambda = \lambda_{cr}$, corresponding to the onset of chaos. Similar changes of the basin structure for $k \to 0$ take place when moving according to the scheme in Fig. 2(a) from top to bottom, from the sole simply connected chaotic attractor to the chaotic attractor of infinite connectivity near the point $\lambda = \lambda_{cr}$.

The introduction of coupling variously affects the structure of basins of attractors having different types of symmetry. Besides the deformation of basins boundaries, the variation of k leads to the redistribution of the area of basins for coexisting attractors. The area of basins of in-phase cycles is increased at the cost of a decrease of the area of basins of out-of-phase cycles. The basins of in-phase cycles therewith become convex, while the basins of out-of-phase cycles become concave (Fig. 6(c)).

All symmetric out-of-phase cycles, for instance, 2_1, demonstrate Hopf bifurcation as the parameter λ increases. The basin of quasiperiodic regime occupies entirely the basin of cycle giving rise to this quasiperiodicity (Fig. 7(a)). The specular symmetric pairs of cycles emerged as the result of frequency locking, for instance, 4_1 and 4_3, divide the torus basin of attraction in such a way, that their basins have equal area (Fig. 7(b)). The way of basins evolution outlined for regular attractors is universal and it is realized for all branches of the scheme in Figs. 1 and 2, corresponding to periodic and quasiperiodic regimes.

The basins of chaotic attractors evolve by a more complicated scheme, depending, in addition on the conditions formulated in [36], and namely, on the location of a certain critical curve in the plane of initial conditions. Let us clarify

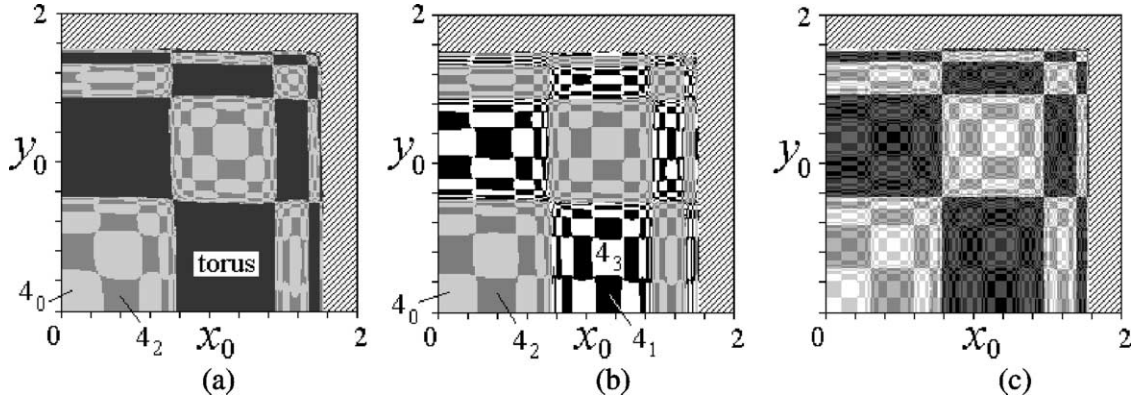

Fig. 7. (a) Basins of attraction of quasiperiodic motions and cycles 4_0 and 4_2 for $\lambda = 1.3$, $k = 0.015$. (b) Basins of attraction of cycles 4_0, 4_1, 4_2, and 4_3 for $\lambda = 1.3$, $k = 0.008$. (c) Basins of attraction of cycles $8_0, 8_1, \ldots, 8_7$ for $\lambda = 1.38$, $k = 0.001$.

the aforesaid. The system (2) belongs to the class of noninvertible maps. The (x, y) plane of this system consists of two open regions Z_0 and Z_4 The points belonging to Z_4 have four preimages (or antecedents) of rank-1, and the points of Z_0 have no real preimages. For instance, the point A in Fig. 5(a) has four A_{-1} preimages, whose coordinates are obtained as the result of the system (2) backward iteration, i.e., after the first iteration the system comes from these points to A. At the same time, the point D has no preimages, because its backward iteration does not fall on the map plot and thus, there are no points in the (x_0, y_0) plane, starting at which the system (2) would come to the point D after the first iteration. The curve which separates the phase plane into two above mentioned regions is called the critical one in [36]. The critical curve can be found by the first iteration of the point set (x_0, y_0), for which the Jacobian of the map vanishes. For the map (2) the critical curve is formed by two rays coming from the point (λ, λ). In Figs. 8 and 9 the critical curve l_{cr} is indicated by dashed lines.

We consider the evolution of chaotic attractors basins depending on their location with respect to the critical curve. For $k \neq 0$ the basins are convex or concave. For the case of weak coupling the typical location of the critical curve is shown in Fig. 8(a) and (b) plotted for the case, when four quadruply connected chaotic attractors exist in the system under investigation. As the parameters vary, the attractors 4^2 and 4^4 merge into the attractor 2^2. The merging of their basins of attraction forms the structure depicted in Fig. 8(c). The attractors 4^1 and 4^3 are slightly changed, but inside almost all elements of their basins of attraction (besides those, containing the attractors themselves) lakes, or holes are formed (Fig. 8(c) and (d)). Here and further we use the geographic analogies suggested by Mira et al. [36]. The appearance of these lakes is explained by forming of the so-called bays, i.e., the closed regions of Z_4 bounded by a segment of l_{cr} and a segment of the basin boundary, the successive preimages of which generate lakes. The existence of an infinite sequence of preimages gives rise to the emergence of an infinite number of lakes. Further parameter variation leads to the formation of islands inside the lakes as the result of the critical curve intersection with the lake (Fig. 8(e) and (f)). Then, inside these islands in turn the embedded lakes are formed, and so on.

Under further variation of parameters λ and k we observe changes unaccountable using the above approach. Attractor 2^2 undergoes a crisis due to its collision with an unstable period-1 cycle and disappears. This is followed by qualitative changes of the region in the (x_0, y_0) plane that previously has belonged to the basin of disappeared attractor: the fractal division of this region into the basins of attractors 4^1 and 4^3 takes place (Fig. 9(a)). As a consequence, the critical curve goes through the fractal set and the nature of its intersection with the basin elements cannot be defined. As for the earlier existing basins of attractors 4^1 and 4^3, they are nonfractal as before: the number of embedded lakes and islands remains a finite magnitude (Fig. 9(b)). But for the values of λ and k higher than certain critical ones these regions structure also becomes fractal and has an infinite number of embeddings (Fig. 9(c) and (d)). The described scenario of basins fractalization is universal and is manifested for chaotic attractors of higher connectivity, but in narrower range of the parameter values.

The features considered above for the basins structure and basins evolution under variation of the parameters are valid for oscillation regimes existing in the region of $k < 0.5$. In the region of greater k values ($k > 0.5$) the basin structure remains intact only for the in-phase and symmetric out-of-phase regimes. Asymmetric regimes have qualitatively different phase portraits for weak and strong coupling, and thus, differently structured basins of attraction. In

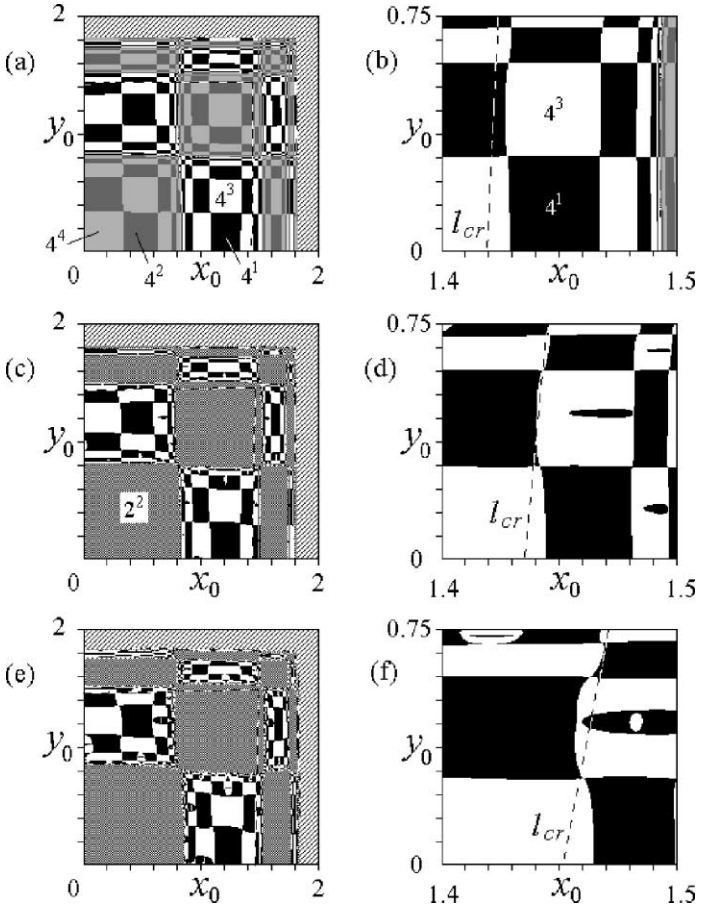

Fig. 8. Formation of lakes in the basins of chaotic attractors 4^1 and 4^3. (a,b) $\lambda = 1.428$, $k = 0.006$, (c,d) $\lambda = 1.454$, $k = 0.0128$, (e,f) $\lambda = 1.49$, $k = 0.025$. The figures at the right are the enlarged fragments of the figures at the left.

Fig. 10(a)–(d) the basins are presented for the regimes existing at the same values of parameter λ as those depicted in Figs. 6(a), 7(b) and (c) and 8(a), respectively. For clearness, the values of coupling in Fig. 10(a)–(d) are chosen as $k = 1 - k_w$, where k_w is the value of coupling in Figs. 6(a), 7(b) and (c) and 8(a), respectively. As it can be seen from Fig. 10(b) and (d) the basins of specular symmetric regimes at strong coupling, in particular, the basins of regimes 4_{I}, 4_{III} and 4^{I}, 4^{III} consist of larger blocks without fractal structure in comparison with the corresponding basins at weak coupling. The fractalization of basins of asymmetric regimes at strong coupling is typical only for regimes N_m and N^m with $N \geqslant 8$ (Fig. 10(c)). As a result, there is no division of the basins of regimes 4^{I} and 4^{III} under variation of the parameters, and the bays, lakes, and islands are not observed. They have to appear for the basins of chaotic attractors of higher connectivity.

The qualitative features of multistable states basins formation considered with the model (2) as an example are typical for a system of symmetrically coupled identical maps having the form (1).

6. Comparison with experiment

We compared the results obtained in the numerical investigation of the discrete system (2) with those obtained in physical experiment with a system of coupled oscillating objects demonstrating transition to chaos via a sequence of period-doubling bifurcations and operating in a continuous time. Driven nonlinear resonators—two *RL*-diode circuits coupled via a resistor, were studied experimentally under in-phase periodic excitation by identical signals using

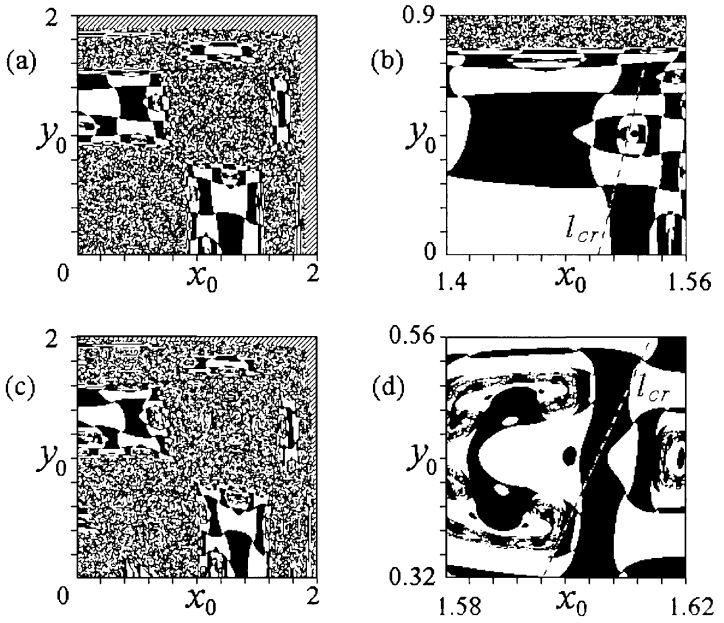

Fig. 9. Basins of chaotic attractors 4^1 (black color) and 4^3 (white color). (a,b) $\lambda = 1.57$, $k = 0.042$, (c,d) $\lambda = 1.7$, $k = 0.07$. The figures at the right are the enlarged fragments of the figures at the left.

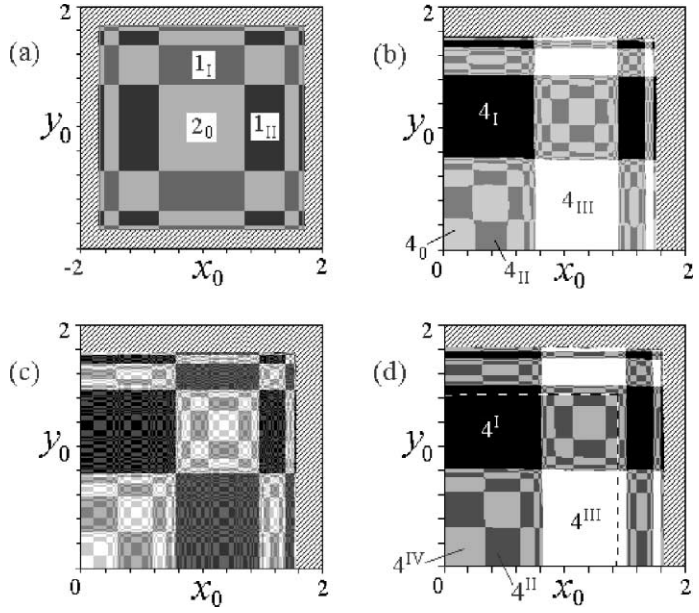

Fig. 10. (a) Basins of attraction of period-1 and period-2 cycles for $\lambda = 1.2$, $k = 1$. (b) Basins of attraction of cycles 4_0, 4_I, 4_{II}, and 4_{III} for $\lambda = 1.3$, $k = 0.992$. (c) Basins of attraction of cycles $8_0, 8_I, \ldots, 8_{VII}$ for $\lambda = 1.38$, $k = 0.999$. (d) Basins of chaotic attractors 4^I, 4^{II}, 4^{III}, and 4^{IV} for $\lambda = 1.428$, $k = 0.994$.

amplifiers (Fig. 11). The conductivity of the coupling resistor $K = 1/R_c$ is the analog of coupling coefficient k. The case $K \to 0$ corresponds to $k \to 0$, and $K \to \infty$ corresponds to $k \to 0.5$. The driving amplitude V is the analog of the pa-

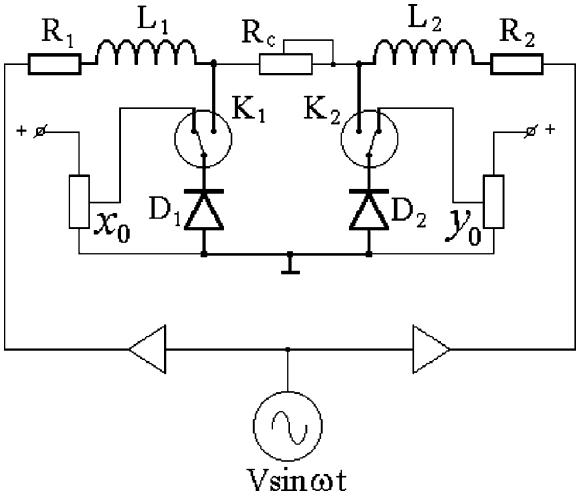

Fig. 11. Scheme of the experimental set. The resonators are indicated by bold lines. R_c is the resistor of coupling, K_1 and K_2 are the electronic keys. $R_1 = R_2$, $L_1 = L_2$ diodes D_1 and D_2 are of the same type.

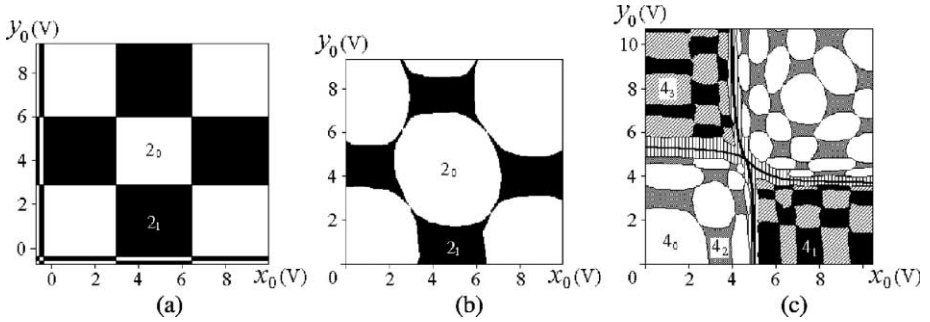

Fig. 12. Basins of attraction of period-2 and period-4 cycles of experimental system. (a) $K = 0$, (b,c) $K \neq 0$.

rameter of nonlinearity λ. Electronic keys K_1 and K_2 were used to set the initial conditions x_0, y_0 These keys connected diodes D_1 and D_2 to additional voltage sources and then restore the circuit so fast, that the distribution of charges in the diodes was not managed to relax to its equilibrium state during the operating time of the keys.

Periodically driven systems as well as point maps are invariant with respect to the discrete group of symmetries. Their oscillations can be classified using the magnitude of the time shift between the subsystem oscillations, which is a multiple of the driving period. The results of our physical experiment are in a good qualitative agreement with those obtained numerically. In particular, for low-period oscillations and $k < 0.5$ all dynamical states of the system (2) are found experimentally. It is shown that the configuration of experimentally obtained bifurcation lines and basins of attraction of various regimes correlate well with the calculated results. In Fig. 12 the two-dimensional projections of experimental basins of attraction for the period-2 and period-4 cycles are shown. The investigated part of the experimental plane (x_0, y_0) is bounded by limits outside which the diodes may be destroyed because of thermal instability. In the absence of coupling $(K = 0)$ the basin elements have a rectangular form (Fig. 12(a)). With the coupling increase, as it is inherent in the model, the in-phase cycle basin expands at the expense of the basin of out-of-phase cycle (Fig. 12(b)). The emergence of additional cycles in the phase space under variation of the parameters leads to the division of all elements of previously existed basins in accordance with the regularities described for the system (2) (Fig. 12(c)). Successive reduction of the basin elements area is observed near the boundary separating the basins of attraction of symmetric cycles 4_0, 4_2 and asymmetric cycles 4_1, 4_3. However, the self-similar basin structure near the boundary cannot be defined in the experiment because of fluctuations and technical restrictions on the scale of resolution. That is why the boundary between the basins of these cycles is indicated by bold line in the figure, and the boundary regions are

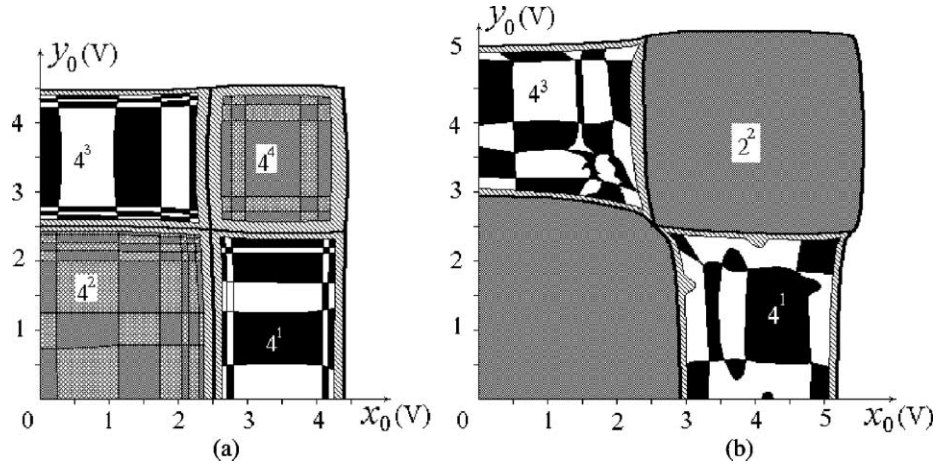

Fig. 13. Basins of the chaotic attractors of experimental system. (a) $V = 1$ V, $K = 0.002$ mS, (b) $V = 1.79$ V, $K = 0.025$ mS.

hatched. The asymmetry of basins about the $x_0 = y_0$ line, observed in the experiment, is due to nonidentity of the real subsystems.

In Fig. 13 the results of the basins experimental examination are presented for quadruply connected chaotic attractors. For weak coupling the basin structure in Fig. 13(a) corresponds qualitatively to that shown in Fig. 8(a). The bold line indicates the boundary separating the basins of chaotic attractors 4^2, 4^4 and 4^1, 4^3. The accumulation of basin elements in the neighbourhood of this line is shown by hatching. The simultaneous variation of driving and coupling parameters induces changes similar to those outlined above for the system (2). The attractors 4^2 and 4^4 merge into the attractor 2^2, and inside the elements of basins of attraction of the regimes 4^1 and 4^3 the lakes are formed (Fig. 13(b)). Under further variation of the parameters the attractor 2^2 undergoes a crisis and disappears. As this takes place, its basin of attraction is divided in a complicated manner into the basins of the attractors 4^1 and 4^3. It may be suggested that fractal structure is formed in this case as well as it takes place in the system (2) (see Fig. 9(a)), but it is impossible to construct this structure in experiment. The form of the transient process and its dependence on natural fluctuations of the experimental system, which leads to unpredictability of establishment of one or another regime, can serve as indirect evidence of the basins fractalization.

7. Discussion

With the system (2) as an example we have shown that a great number of multistable states exist in the parameter space of symmetrically coupled identical systems and the basins of attraction of these states have sufficiently complicated arrangement. The establishment of one or another oscillating regime is defined both by the parameter values and the initial conditions, what is illustrated by the presented schemes. Consequently, the change of regimes under variation of one of the parameters is defined by the location of initial point in the phase space and by the evolution of basin boundaries.

The obtained results can be useful when solving the problem of synchronization of nonlinear systems and simplification and regularization of their dynamics by introducing an appropriate coupling. Basing on the scheme of regimes it can be stated, for instance, that the existence of the so-called seven-zone dynamics [35], i.e., that of a sequence of regimes of complex–periodic–chaotic out-of-phase–chaotic in-phase–chaotic out-of-phase–periodic–complex behavior under variation of the coupling parameter from zero to unity, is not a universal property for coupled maps with negative Schwartzian curvature, as it has been believed in [35]. The number of zones used for classification of coupled dynamics under variation of coupling depends on other parameter values and on the choice of initial conditions. In particular, the number of zones can be 5, 7, 9, 11. In Fig. 14 the difference of subsystem oscillations is plotted against the coupling parameter. Zones 1 and 9 in Fig. 14(a) are regions of complex, mostly chaotic dynamics. Zones 2, 4 and 8, 6 are characterized by periodic behavior. The complex (quasiperiodic) behavior is observed in both zone 3 and zone 7. Zone 5 corresponds to synchronous chaotic behavior. In Fig. 14(b) the complex behavior is observed in zones 1 and 5.

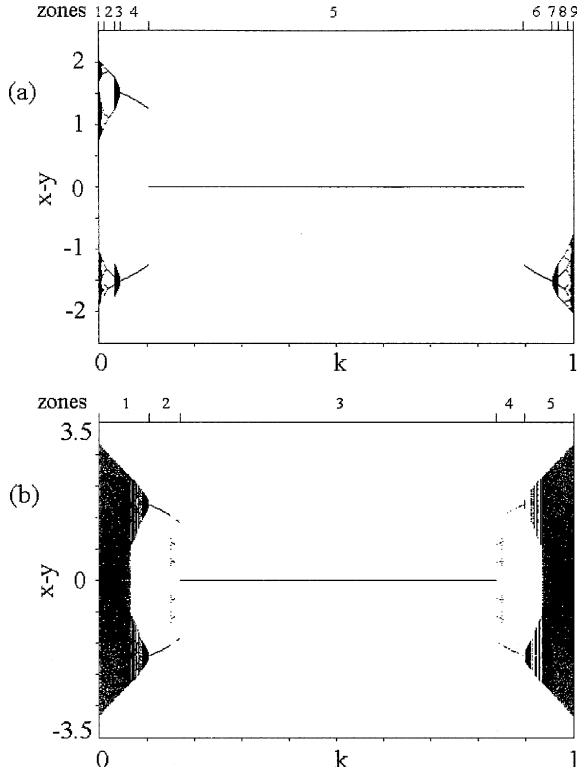

Fig. 14. (a) The nine-zone dynamics for the system (2) for $\lambda = 1.42$ and initial conditions $(x_0, y_0) = (0, 1)$. (b) The five-zone dynamics for $\lambda = 1.74$, $(x_0, y_0) = (0, 1)$. For each k value 1000 sequential values of the difference $x - y$ are plotted after discarding 50,000 initial iterations.

Zones 2 and 4 are regions of periodic oscillations. Zone 3 is a region of chaotic in-phase behavior. It should be noted that regions of chaotic out-of-phase behavior are absent under the chosen initial conditions and λ values. Under the exchange $x_0 \leftrightarrow y_0$ the plots in Fig. 14 reflect about the $(x - y) = 0$ line. The notion of the mutual arrangement of co-existing attractors and their evolution under variation of the parameters allows us to conclude that a quasiperiodic transition to chaos, typical for a system of symmetrically weakly coupled maps [7], already disappears at relatively small values of the coupling coefficient.

The obtained in our work results are common for a wide class of systems (1) under the condition of identity between unimodal functions $f(x_n)$ and $f(y_n)$. In the case of multimodal functions $f(x_n)$ and $f(y_n)$ the variety of the system (1) oscillation states becomes greater. The oscillations of subsystems can significantly differ even at zero coupling if the isolated elements possess bistability and their initial conditions are chosen from the basins of attraction of different states. As a result, additional sheets appear in the scheme depicted in Fig. 1.

A close qualitative agreement between the results of discrete modeling and those of physical experiment points to the commonness of the represented scheme of regimes for dissipatively coupled systems. The merits of the suggested description of oscillation types are confirmed by the results of experiments with coupled period-doubling systems for other types of coupling and excitation [37,38]. In these cases the internal structure of sheets in the (k, λ) plane is conserved, therewith the size and mutual arrangement of sheets are defined by the type of coupling.

Acknowledgements

This work was supported by the Russian Foundation of Fundamental Research, grant no. 02-02-17578 and by US Civilian Research Development Foundation for the Independent States of the Former Soviet Union, Award no. REC-006.

References

[1] Frøyland J. Some symmetric, two-dimensional, dissipative maps. Physica D 1983;8:423–34.
[2] Kaneko K. Similarity structure and scaling property of the period-adding phenomena. Prog Theor Phys 1983;69:403.
[3] Yuan J-M, Tung M, Feng DH, Narducci LM. Instability and irregular behavior of coupled logistic equations. Phys Rev A 1983;28:1662.
[4] Buskirk R, Jeffries C. Observation of chaotic dynamics of coupled nonlinear oscillators. Phys Rev A 1985;31:3332–57.
[5] Sakaguchi H, Tomita K. Bifurcations of the coupled logistic map. Prog Theor Phys 1987;78:305–15.
[6] Satoh K. Quasiperiodic route to chaos in a coupled logistic map. J Phys Soc Jpn 1991;60:718–9.
[7] Reick C, Mosekilde E. Emergence of quasiperiodicity in symmetrically coupled, identical period-doubling systems. Phys Rev E 1995;52:1418–35.
[8] Kuznetsov SP. Universality and similarity in the behavior of coupled Feigenbaum systems. Izv Vyssh Uchebn Zaved Radiofiz 1985;28:991–1007.
[9] Satoh K, Aihara T. Self-similar structures in the phase diagram of a coupled-logistic map. J Phys Soc Jpn 1990;59:1123–6.
[10] Kook H, Ling FH, Schmidt G. Universal behavior of coupled nonlinear systems. Phys Rev A 1991;43:2700–8.
[11] Kim S-Y. Universal scaling in coupled maps. Phys Rev E 1995;52:1206–9.
[12] Ferretti A, Rahman NK. Coupled logistic maps in physico-chemical processes: coexisting attractors and their applications. Chem Phys Lett 1987;140:71–5.
[13] Astakhov VV, Bezruchko BP, Gulyaev YuV, Seleznev YeP. Multistable states of dissipatively coupled Feigenbaum systems. Pis'ma Zh Tekh Fiz 1989;15:60–5.
[14] Astakhov VV, Bezruchko BP, Erastova EN, Seleznev YeP. Types of oscillation and their evolution in dissipatively coupled Feigenbaum systems. Zh Tekh Fiz 1990;60:19–26.
[15] Astakhov VV, Bezruchko BP, Pudovochkin OB, Seleznev YeP. Phase multistability and transition to oscillation steady in nonlinear systems with period-doubling. Radiotekh Elektron (Moscow) 1993;38:291–5.
[16] Prokhorov MD. Oscillation types of dissipatively coupled period-doubling systems at strong coupling. Izv Vyssh Uchebn Zaved Prikl Nelin Dinam 1996;4:99–107.
[17] Carvalho R, Fernandez B, Mendes RV. From synchronization to multistability in two coupled quadratic maps. Phys Lett A 2001;285:327–38.
[18] Gu Y, Tung M, Yuan JM, Feng DH, Narducci LM. Crises and hysteresis in coupled logistic maps. Phys Rev Lett 1984;52:701–4.
[19] Metzler W, Beau W, Frees W, Ueberla A. Symmetry and self-similarity with coupled logistic maps. Z Naturforsch A 1987;42:310–8.
[20] Inoue M, Nishi Y. Highly complicated basins of periodic attractors in coupled chaotic maps. Prog Theor Phys 1996;95:685–90.
[21] Bezruchko BP, Seleznev YeP. Basins of attraction for chaotic attractors in coupled systems with period-doubling. Pis'ma Zh Tekh Fiz 1997;23:40–6.
[22] Anishchenko VS. Dynamical chaos in physical systems. Leipzig: Teubner; 1989.
[23] Gyllenberg M, Soderbacka G, Ericsson S. Does migration stabilize local population dynamics? Analysis of a discrete metapopulation model. Math Biosci 1992;118:25.
[24] Bezruchko BP, Prokhorov MD, Seleznev YeP. Features of the parameter space structure for a system of two coupled nonautonomous nonisochronous oscillators. Pis'ma Zh Tekh Fiz 1996;22:61–6.
[25] Yamada T, Fujisaka H. Stability theory of synchronized motion in coupled-oscillator systems. II. The mapping approach. Prog Theor Phys 1983;70:1240.
[26] Pikovsky AS. On the interaction of strange attractors. Z Phys B 1984;55:149–54.
[27] Kuznetsov SP, Pikovsky AS. Symmetry breaking bifurcation in the system of dissipatively coupled recurrent mappings. Izv Vyssh Uchebn Zaved Radiofiz 1989;32:49–54.
[28] Pikovsky AS, Grassberger P. Symmetry breaking bifurcation for coupled chaotic attractors. J Phys A 1991;24:4587–97.
[29] Astakhov V, Shabunin A, Kapitaniak T, Anishchenko V. Loss of chaos synchronization through the sequence of bifurcations of saddle periodic orbits. Phys Rev Lett 1997;79:1014–7.
[30] Kapitaniak T, Maistrenko YL. Chaos synchronization and riddled basins in two coupled one-dimensional maps. Chaos, Solitons & Fractals 1998;9:271–82.
[31] Yang HL, Pikovsky AS. Riddling, bubbling, and Hopf bifurcation in coupled map systems. Phys Rev E 1999;60:5474–8.
[32] Maistrenko YuL, Maistrenko VL, Popovich A, Mosekilde E. Transverse instability and riddled basins in a system of two coupled logistic maps. Phys Rev E 1998;57:2713–24.
[33] Maistrenko YuL, Maistrenko VL, Popovych O, Mosekilde E. Desynchronization of chaos in coupled logistic maps. Phys Rev E 1999;60:2817–30.
[34] Popovych O, Maistrenko Yu, Mosekilde E, Pikovsky A, Kurths J. Transcritical riddling in a system of coupled maps. Phys Rev E 2001;63:036201.
[35] Udwadia FE, Raju N. Some global properties of a pair of coupled maps: quasi-symmetry, periosynchronicity synchronicity. Physica D 1998;111:16–26.
[36] Mira C, Fournier-Prunaret D, Gardini L, Kawakami H, Cathala JC. Basin bifurcations of two-dimensional noninvertible maps: fractalization of basins. Int J Bif Chaos 1995;4:343–81.

[37] Astakhov VV, Bezruchko BP, Kuznetsov SP, Seleznev YeP. Features of quasiperiodic motion occurrence in a system of dissipatively coupled periodically driven nonlinear oscillators. Pis'ma Zh Tekh Fiz 1988;14:37–41.
[38] Astakhov VV, Bezruchko BP, Ponomarenko VI, Seleznev YeP. Multistability in a system of radiotechnical oscillators with capacitive coupling. Radiotekh Elektron (Moscow) 1991;36:2167–70.